frontiers | Frontiers in Astronomy and Space Sciences

TYPE Review
PUBLISHED 17 September 2024
DOI 10.3389/fspas.2024.1471140

OPEN ACCESS

EDITED BY
David Hysell,
Cornell University, United States

REVIEWED BY
Vladimir Truhlik,
Institute of Atmospheric Physics (ASCR), Czechia
Yong-Qiang Hao,
Sun Yat-sen University, China

*CORRESPONDENCE
Bela G. Fejer,
bela.fejer@usu.edu

RECEIVED 26 July 2024
ACCEPTED 27 August 2024
PUBLISHED 17 September 2024

CITATION
Fejer BG, Navarro LA and Chakrabarty D (2024) Recent results and outstanding questions on the response of the electrodynamics of the low latitude ionosphere to solar wind and magnetospheric disturbances.
Front. Astron. Space Sci. 11:1471140.
doi: 10.3389/fspas.2024.1471140

Recent results and outstanding questions on the response of the electrodynamics of the low latitude ionosphere to solar wind and magnetospheric disturbances

Bela G. Fejer[1]*, Luis A. Navarro[2] and Dibyendu Chakrabarty[3]

[1]Center for Atmospheric and Space Sciences, Utah State University, Logan, UT, United States, [2]Space Weather, Technology, and Education Center, University of Colorado, Boulder, CO, United States, [3]Space and Atmospheric Sciences Division, Physical Research Laboratory, Ahmedabad, India

Storm-time ionospheric electrodynamics effects have been the subject of extensive studies. The solar wind/magnetosphere/ionosphere and thermosphere disturbance wind dynamos have long been identified as the main drivers of low latitude storm-time electrodynamics. Extensive detailed studies showed that climatology of low latitude disturbance electric fields and currents is in good agreement with results from global theoretical and numerical models. Over the last decade, however, numerous studies have highlighted that the response of low latitude electrodynamics to enhanced geomagnetic activity is significantly more complex than previously considered. It is now clear that the electrodynamic disturbance processes are affected by a larger number of solar wind and magnetospheric parameters and that they also have more significant spatial dependence. This is especially pronounced during and after large geomagnetic storms when multiple simultaneous disturbance processes are also active. In this work, we briefly review the main past experimental and modeling studies of low latitude disturbance electric fields, highlight new results, discuss outstanding questions, and present suggestions for future studies.

KEYWORDS

geomagnetic storms and substorms, magnetospheric effects on low latitude ionosphere, electrodynamics response to solar wind disturbances, electrodynamics response to magnetospheric disturbances, low latitude ionosphere

1 Introduction

The response of electrodynamics of the low latitude ionosphere to enhanced geomagnetic activity has long been subject of numerous studies. Starting in the late 1970s, it was clearly established that the solar wind magnetosphere and the ionosphere disturbance wind dynamos are the main processes driving storm-time global ionospheric electric field and current perturbations. The solar wind magnetospheric dynamo drives short-lived (up to a few hours) so-called prompt penetration electric fields processes resulting from the leakage of high-latitude potential to lower latitudes when there is a temporary imbalance between region 1 and region 2 Birkeland currents (e.g., Wolf, 1970;

Kelley et al., 1979; Senior and Blanc, 1984; Spiro et al., 1988; Sazykin, 2000; Huang C.-S. et al., 2007; Wolf et al., 2007; Fejer et al., 2007; Fejer, 2011; Chakrabarty et al., 2015). Shorter-lived ionospheric prompt penetration electric fields and currents extending down to equatorial latitudes are also often driven by magnetospheric substorms (e.g., Kikuchi, 2000; Kikuchi et al., 2008; Chakrabarty et al., 2008; 2015; Wei et al., 2009; Wei et al., 2015; Huang C.-S., 2009; Fejer et al., 2021; 2024), solar wind dynamic pressure changes (e.g., Rout et al., 2019; Huang C.-S., 2020; Le et al., 2024), solar flares (e.g., Zhang R. et al., 2017) and ULF waves (e.g., Huang C.-S., 2020). The thermosphere disturbance dynamo, generated by storm-time enhanced energy and momentum deposition into the high-latitude ionosphere, drives longer lasting (up to a few days) global ionospheric electric field and current perturbations (e.g., Blanc and Richmond, 1980; Scherliess and Fejer, 1997; Fejer et al., 2017; Pandey et al., 2018; Navarro et al., 2019). Storm and post-storm prompt penetration and disturbance electric fields cause large perturbations on low latitude thermospheric winds, composition, and plasma density, and affect the occurrence of low latitude plasma irregularities (e.g., Fejer et al., 1999; Chakrabarty et al., 2006; Balan et al., 2008; Fuller-Rowell al., 2008; Fagundes et al., 2016; Xiong et al., 2015; Heelis and Maute, 2020; Navarro and Fejer, 2020).

The climatology of low latitude prompt penetration and disturbance electric fields has been known for over 2 decades, but there is still very little information on their temporal and longitudinal variations [e.g., Abdu, 2016; Abdu et al., 2007; Fejer and Maute, 2021]. Recent studies reported large spatial/temporal changes on disturbance electric fields due, for example, to IMF By changes, season, hemispheric dependent high latitude convection rotations and skewings, and to polar electrojet effects. Furthermore, as pointed out by Dick Wolf (private communication, 2022): "For the last 15 years or so, it has become very clear that plasma distributions are not approximately constant along the plasma sheet tailward boundary, as assumed by old style convection models. As a result, bubbles of depleted plasma sporadically occurring in the plasma sheet, probably because of reconnection, can sometimes make their way deep into the inner magnetosphere". Highly dynamic related processes, such as auroral streamers and substorms (e.g., Yadav et al., 2023), likely cause the electrodynamic response of the low latitude ionosphere to geomagnetic activity to be much richer and complex than previously thought. In the meantime, global ionospheric storm time models have recently undergone major improvements and now have increasingly been used in global simulations of complex storm events.

In the following sections, we first describe recent findings on the effects of solar wind, magnetospheric and high latitude drivers on low latitude ionospheric electric fields and currents. We also discuss recent studies of high latitude electrodynamics that are likely to affect the electrodynamics of the low latitude ionosphere. Next, we illustrate the complex longitude dependent response of equatorial ionospheric electrodynamic electric fields during extended periods of high geomagnetic activity emphasizing the challenges in effects of individual storm drivers. We then summarize recent results on low latitude storm-time modeling. Finally, we highlight outstanding questions and present suggestions for improving our understanding of this complex subject.

2 Drivers of low latitude storm-time electrodynamics

2.1 IMF Bz effects

The north-south (Bz) component of IMF is the most important driver of dayside reconnection and of solar wind, magnetosphere coupling (e.g., Wolf, 1970). Polarity changes in IMF Bz have long been known as the main drivers of low latitudes storm-time ionospheric disturbances. As extensively documented, southward (northward) IMF Bz excursions faster than shielding time constant (~30 min) drive undershielding (overshielding) electric fields. These electric fields cause upward/westward (downward/eastward) prompt penetration equatorial plasma drifts during the day and with opposite polarity at night with peak values near the terminators (e.g., Fejer et al., 1990; Fejer et al., 1997; Huang C.-S., 2015; Kikuchi and Hashimoto, 2016). Slower Bz turnings do not give rise to significant penetration of electric fields. Regression analysis of IMF Bz and conductivity-corrected equatorial electrojet data suggests higher prompt penetration efficiency during northward than southern turnings (Bhaskar and Vichare, 2013). The ratio of the equatorial zonal penetration and the motional solar wind (dawn-dusk) electric fields is ~0.1 during the day (e.g., Kelley et al., 2003; Huang C.-S. et al., 2010; Huang C.-S. et al., 2010; Manoj et al., 2012) and larger near sunrise and sunset (e.g., Fejer and Scherliess, 1997; Wei et al., 2008; Fejer, 2011). The amplitudes of the meridional/perpendicular prompt penetration electric fields are about twice larger (e.g., Sazykin, 2000; Fejer and Emmert, 2003; Huang C.-S. et al., 2010). These ratios vary with solar wind and magnetospheric parameters (e.g., Spiro et al., 1988; Garner et al., 2004) and under the effect of additional solar wind (e.g., dynamic pressure) and magnetospheric (e.g., substorms) processes.

The lifetimes of Prompt penetration electric fields associated with rapid southward IMF Bz turnings faster are generally ~1–2 h [e.g., Fejer and Scherliess, 1997; Manoj and Maus., 2012], although much longer values (up to ~10 h) have also been suggested (e.g., Huang C.-S., et al., 2010a; Huang C.-S., et al., 2010b). For slowly varying southward IMF Bz conditions, short-lived prompt penetrations equatorial electric fields can be driven by magnetospheric substorms, changes in IMF By, and solar wind dynamic pressure changes. This is illustrated in Figure 1 with F-region vertical plasma drift measurements over Jicamarca, Peru (11.9°S, 76.8°W; dip latitude ~0°). Over this site, eastward/downward electric fields of 1 mV/m correspond to upward/westward drifts of ~40 m/s. Equatorial storm time electric fields during extended periods of southward IMF Bz will be discussed in detail later.

Rout et al. (2022) presented evidence for quasiperiodic (1.5–2 h) fluctuations in low latitude ionospheric electric fields, solar wind zonal electric field and global geomagnetic fluctuations during High-Intensity Long-Duration Continuous AE Activity (HILDCAA) events. Recently, Milan et al. (2023) concluded that the AE/AL disturbances during HILDCAAs are caused by high-intensity quasi-periodic substorms driven by high but intermittent dayside reconnection rate due to fast solar wind and quasi-periodically varying IMF. Low latitude ionospheric electric fields during these events, however, should also be directly affected by IMF Bz sign fluctuations.

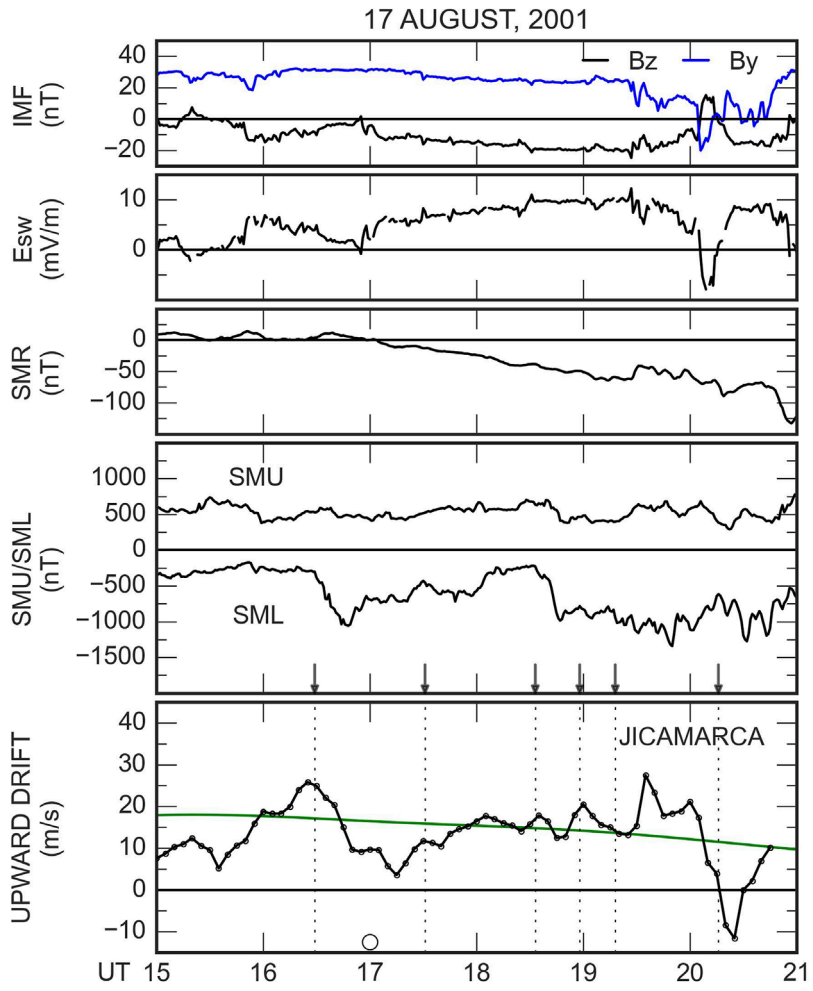

FIGURE 1
(From top to bottom) IMF Bz/By, solar wind motional east-west electric field, SuperMAG ring current (SMR) and auroral current (SMU/SML) indices with substorm onset times (small arrows in the bottom panel), Jicamarca vertical plasma drifts during the initial phase of the 17 August 2001slowly developing magnetic storm. The smooth curve denotes the quiet-time drift pattern.

Even though prompt penetration effects are most often associated with IMF Bz turnings and southward conditions, it has been known for some time that this is not always the case. Recent studies have reexamined earlier investigations (e.g., Kelley and Makela, 2002; Zhao B. et al., 2008) of equatorial prompt penetration electric fields and currents lasting longer than a few hours under northward IMF (NBz) and duskward (By > 0) conditions. Li et al. (2023) discussed one such event in connection with energy deposition at higher latitudes than under southward IMF Bz. They also showed that Thermosphere-Ionosphere-Electrodynamics General Circulation Model (TIE-GCM) simulations reproduced the observed changes in high latitude convection, Joule heating and thermospheric winds, as well as resulting low latitude westward prompt penetration electric fields. Wang and Luhr (2024) presented extensive CHAMP and Swarm measurements showing that, under long-duration NBz, the polar electrojet driven low-high latitude ionospheric electrodynamical coupling is strongly dependent on IMF By sign, local time, and season.

2.2 IMF By effects

The dawn-dusk (By) component of IMF modulates the dayside reconnection rate and affects the ionospheric convection patterns (e.g., Heelis, 1984; Cunnock et al., 1992). Tsurutani et al. (2008) pointed out that the polarity of equatorial prompt penetration electric field perturbations near dawn and dusk could be affected due to possible skewing and asymmetry between the DP2 convection vortices. Tenfjord et al. (2015) described the role of IMF By on asymmetric currents, convection patterns and substorm onset locations in the two hemispheres (e.g., Østgaard et al., 2004; 2011). Only recently have IMF By effects on the electrodynamics of the low latitude ionospheric have been studied in detail.

Chakrabarty et al. (2017) suggested that unusual equatorial prompt penetration electric fields with identical polarity near dawn and dusk over nearly antipodal stations in Indian and South American could be explained as resulting from IMF By driven asymmetric and skewed DP2 current lobes. This role of IMF By under southward Bz is also supported by consistently

observed (e.g., Kumar et al., 2023; Chakraborty and Chakrabarty, 2023) high latitude out-of-phase and low latitude in-phase variations of the geomagnetic X component over the antipodal stations corresponding to longitudes in the day and night sectors. We note that asymmetric and distorted high latitude currents should also have major spatial and temporal effects on equatorial disturbance dynamo electric fields.

It is now evident that, contrary to what has been generally assumed, the dependence of auroral currents on IMF By is not symmetric with respect with its sign (e.g., Friis-Christensen et al., 1972; 1985). This dependence is particularly strong in the AL index and during the solstices. During northern hemisphere winter (i.e., under negative tilt angle of the Earth's magnetic dipole relative to the Sun-Earth line), for example, the northern AL index can ~40% stronger for By > 0 than for By < 0. Holappa and Buzulukova (2022) suggested that this interhemispheric effect can be accounted for in the Newell et al. (2007) solar wind magnetosphere coupling function dF_{MP}/dt through $(1 - 0.04\,By \tan \psi)$, where ψ is the dipole tilt angle and By is nT. Reistad et al. (2022) reported more frequent substorm occurrence when IMF B_y and dipole tilt have opposite signs. This was attributed to a more efficient global dayside reconnection rate. We note in passing that Cowley (1981), Cowley et al. (1991) and Laundal and Ostgaard (2009) suggested stronger and more efficient solar wind dynamo in the southern hemisphere under large positive IMF Bx. The hemispheric asymmetries caused by IMF By and possibly IMF Bx should play a major role on the spatial and temporal variability of both equatorial prompt penetration and disturbance electric fields near sunrise and sunset, particularly during the solstices.

There are other aspects regarding IMF By effects on equatorial disturbance electric fields remain unclear such as what proportion of IMF Bz and IMF By is the most effective one and whether a stable and significantly high IMF By is more effective than the polarity reversal in IMF By or *vice versa*. In the absence of modelling and clinching evidence, one should not discard the role of any of the above factors *ab initio*.

2.3 Solar wind density and dynamic pressure effects

Increased solar wind dynamic pressure causes magnetospheric compression and drives enhanced the two-cell convection and DP-2 currents (e.g., Liou et al., 2017). In the daytime equatorial ionosphere, they give rise to short-lived (~30 min) upward and westward plasma drift perturbations (e.g., Fejer and Emmert, 2003; Huang C.-S., 2020; Nilam et al., 2020). Sharp dynamic pressure decreases cause prompt penetration electric fields with opposite polarity (e.g., Le et al., 2024). These polarities do not appear to depend on the directions of IMF Bz and By (Nilam et al., 2020). Earlier, Wei et al. (2012) illustrated the control of the equatorial prompt penetration electric field by the solar wind density during a saturation of cross the polar cap potential, and Rout et al. (2016) reported brief (~30 min) simultaneous increases in the high-latitude convection and electric equatorial electric fields under northward IMF Bz after an increase in the solar wind density. Similar effects in equatorial plasma drifts and thermospheric winds were reported by Navarro and Fejer (2020) following solar wind dynamic pressure increases.

2.4 Substorm effects

Induction electric fields resulting from magnetospheric substorm dipolarizations (e.g., Wolf et al., 1982) are increasingly been recognized as important drivers of short-lived (~0.5 h) equatorial prompt penetration electric fields and currents (Kikuchi et al., 2003; Wei et al., 2009; Huang C.-S, 2012; Chakrabarty et al., 2010; 2015; Hui et al., 2017; Tulasi Ram et al., 2016; Fejer et al., 2021; 2024; Kikuchi, 2021; Sori et al., 2022; Fejer and Navarro, 2022). Magnetospheric substorms always occur when IMF Bz is southward for over ~2 h after its southward turning (e.g., Caan et al., 1977). They are often associated with changes in the solar wind drivers including IMF polarity reversals), sharp changes in the solar wind ram pressure, and with internal magnetospheric triggers (Liou et al., 2018). MHD simulations (Tanaka et al., 2010; Ebihara et al., 2014) showed that during substorms, region-2 field aligned currents driven by anisotropic plasma pressure in the inner magnetosphere can cause overshielding-like effects (i.e., daytime westward electric fields). Liou et al. (2020) reported that, on average, there are ~1/3 more substorms for IMF By > 0 than for IMF By < 0, which was attributed to the asymmetry in enhanced convection.

Substorm onset and expansion phases have been associated with both eastward (e.g., Hui et al., 2017; Huang C.-S., 2020) and westward (Kikuchi et al., 2003; Hui et al., 2017) daytime equatorial prompt penetration electric fields. A statistical analysis of disturbed equatorial electrojet using AE index by Yamasaki and Kosch (2015) indicates that the average equatorial electrojet perturbation electric field associated with substorm onset is eastward and lasts for 30–60 min. Their derived short-and long-term climatological responses of the electrojet to substorms are consistent with Jicamarca prompt penetration and disturbance dynamo electric field patterns. Gao et al. (2023) also reported substorm driven prompt penetration and disturbance dynamo patterns consistent with previous results. As mentioned earlier, substorms often occur during periods of changing solar wind parameters and, therefore, it is usually difficult to isolate their contributions to penetration electric fields.

Jicamarca radar drift measurements during periods of nearly steady southward IMF Bz and By and small changes in the solar wind dynamic pressure strongly suggest that substorm onsets and expansion phases (recovery phases) are mostly associated with eastward/poleward (westward/equatorward) prompt penetration electric fields during daytime-evening and with opposite polarities at night. This is consistent with plasma sheet heating and resulting in reduction in shielding during substorm expansion phase (Baumjohann et al., 1996). The eastward and westward perturbation electric fields during onset-expansion and recovery phase often appear to have comparable lifetimes and amplitudes, as in the case of longer lasting (~3 h) equatorial electric fields during the so-called sawtooth events (Huang C.-S., 2012). Substorm driven equatorial vertical drifts are generally small (less than ~5–10 m/s) during the day.

Figure 2 presents in the top 5 panels the IMF Bz/By, solar motional electric field and dynamic pressure, and the SMR,

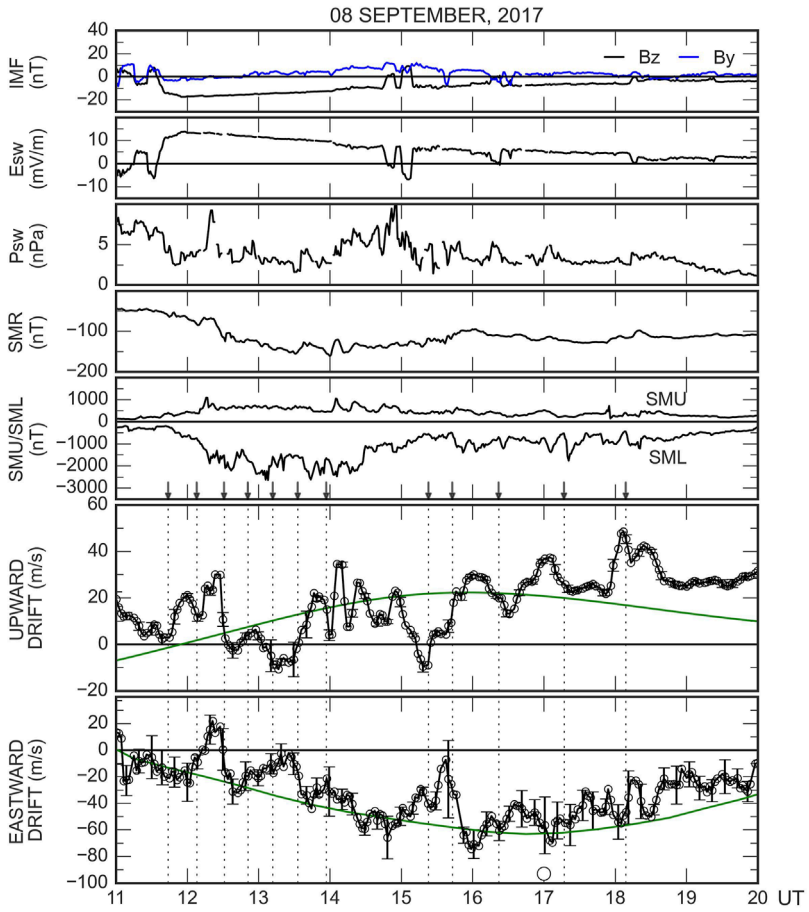

FIGURE 2
(Top five panels) solar wind IMF Bz/By, motional east-west electric field and dynamic pressure, and SuperMAG ring current (SMR) and auroral current (SMU/SML) indices with and substorm onset times (small arrows). (Bottom panels) Height averaged Jicamarca vertical and zonal plasma drifts. The circle at 17 UT indicates noon over Jicamarca and the green curves denote the quiet time vertical and zonal drift patterns (adapted from Fejer and Navarro, 2022).

SMU, and SML indices, and in the two bottom panels, the daytime vertical and zonal F-region vertical drifts measured over Jicamarca during the mostly steady southward IMF Bz period encompassing the second main and recovery phases of the September 2017 large geomagnetic storm. This Figure shows upward/westward perturbation drifts during periods of slowly varying southward IMF Bz and solar wind dynamic pressure, and two large overshielding events at ~12:30–13:30 UT and 15:00–16:00 UT. The first, which occurred after increase in the solar wind dynamic pressure, could be interpreted as resulting from the substorm associated process increased Region 2 Field-Aligned Currents (R2 FACs) caused by inner magnetospheric anisotropic plasma pressure (e.g., Ebihara et al., 2014). This process will be discussed further later. The second overshielding event, shown in Figure 2, occurred during substorm activity following rapid fluctuations in the solar wind dynamic pressure and IMF Bz sign. Yadav et al. (2023) associated dayside and nightside equatorial electrojet overshieldings with equatorward extending streamers resulting from plasma sheet burst flows. They suggested that these auroral streamers, which can be associated with sharp decreases in the SML index, cause overshieldings also by strenghtening Region 2 Field-Aligned Currents (R2 FACs) over R1 FACs.

The low latitude ionospheric typical electrodynamic response to long-lasting southward IMF Bz-driven geomagnetic storms is the nearly continuous occurrence of short-lived (time scales ~30–60 min) substorm-driven prompt penetration electric fields. This was the case, for example, of the equatorial electrojet response to the CME driven July 2012 large geomagnetic studied in detail by Bagiya et al. (2014), Liu et al. (2014), Kuai et al., 2017. In this event, over a period of about 30 h of slowly varying southward IMF Bz, SuperMAG identified 30 substorms, which gave rise to the observed daytime short-lived equatorial electrojet eastward current perturbations, including under strong disturbance dynamo conditions (Figure 5 in Liu et al., 2014). Substorm-driven prompt penetration electric fields under strong disturbance dynamo electric fields were also reported by Fejer et al. (2024). Low latitude electrodynamic signatures during long-lasting southward IMF Bz will be discussed further later.

Substorm associated equatorial prompt penetration electric fields often have very large amplitudes (over ~100 m/s) near

dusk (e.g., Fejer et al., 2021; 2024). Figure 3 shows solar wind, magnetospheric, and high latitude ionospheric parameters, and Jicamarca vertical drifts and coherent backscattered power from 3-m plasma irregularities close to dusk during 27–28 August 2015. This was a period of moderate recurrent geomagnetic activity when the solar wind electric fields (~3 mV/m) were typically too small for directly driving noticeable equatorial prompt penetration electric fields. These substorm associated prompt penetration electric fields caused one of the largest dusk side upward drift perturbations (~60 m/s) ever recorded over Jicamarca during June solstice (Fejer et al., 2021). The large and sudden backscattered power decrease at ~00:15 UT is indicative of strong westward prompt penetration electric fields associated with substorm recovery. Substorm associated prompt penetration electric fields near dusk are most easily identified during periods of small prereversal velocity enhancements, i.e., primarily near June solstice over Jicamarca. Fejer et al. (2008) reported that this is also the season with highest amplitude prompt penetration electric fields near the terminators.

2.5 Solar flare effects

Sudden increases in solar X-ray and Extreme Ultraviolet (EUV) radiation during solar flares lead to large and rapid ionospheric changes (e.g., Tsurutani et al., 2020). Low latitude solar flare effects were discussed in several papers (e.g., Qian et al., 2012; Fejer and Maute, 2021). Zhang K. et al. (2021) reported solar associated increases in daytime eastward equatorial electrojet current and simultaneous decreases in the eastward electric fields, as indicated by Jicamarca vertical drifts. They suggested that the eastward electric field decreases may be due to disturbed ionospheric dynamo caused by flare enhanced Cowling conductivity and perhaps also to overshielding effects. Pedatella et al. (2019) and Chen et al. (2021) presented numerical simulations of sudden daytime equatorial upward drifts (eastward electric field) decreases similar to Jicamarca observations after flare onsets. The simulations of Chen et al. (2021) also indicate that solar flares increase global daytime currents and reduce the eastward electric fields extending from the equator to middle latitudes. Both simulations suggest that the above electrodynamic effects resulted largely from flare-induced conductivity enhancements; prompt penetration electric field effects were not considered.

2.6 SAPS/SAID effects

The occurrence of large poleward-directed electric fields in the evening sub-auroral ionosphere was first pointed out by Galperin et al. (1974) who called them Polarization Jets (PJs). Similar intense narrow electric field structures were called Sub-Auroral Ion Drifts (SAIDs) (Spiro et al., 1979). These two structures and the longer lasting broader latitudinal region of intense sunward plasma drift (e.g., Yeh et al., 1991), are now commonly referred to as Sub-Auroral Polarization Streams (SAPS) (e.g., Foster and Burke, 2002; Foster and Vo, 2002). SAPS are characteristic features of the low conductivity subauroral region during the main and recovery phases of strong magnetic storms (e.g., Foster and Burke, 2002; Foster and Vo, 2002). These poleward electric fields are caused by the separation of the ion and electron plasma sheet edges in the magnetosphere. Huang C.-S et al. (2020b) presented Defense Meteorological Satellite Program (DMSP) satellite measurements showing SAPS peak westward velocities highly correlated with Dst index lasting up to 2 days during both the storm main phase with southward IMF and recovery phase with northward IMF. Huang C.-S et al. (2021) suggested that during very large storms SAPS plasma flows/electric fields near dusk penetrate to the equatorial region driving peak westward plasma drifts of up to 200–300 m/s. They these disturbance drifts related to Dst approximately (correlation 0.87) through $\Delta V = 0.52$ Dst, where 0.52 Dst is in nT. The DMSP equatorial vertical drift measurements during these periods were not discussed. Jicamarca radar measurements during the 22–23 April 2023 geomagnetic storm presented by Fejer et al. (2024) show ~100 m/s westward disturbance drifts near dusk under large, nearly steady, southward IMF Bz and SMR~120 nT, Dst~100 nT conditions. During this period, the vertical drifts had very large amplitude fluctuations typical of substorm driven prompt penetration electric fields.

Huang C.-S et al. (2021) reported CHAMP satellite measurements close to midnight showing large westward disturbance winds rapidly (within 2 h) extending down to equatorial latitudes, and DMSP measured eastward drifts extending down to ~20° magnetic latitudes at 0930 LT. Huang C.-S. (2020) suggested that SAPS associated equatorial zonal disturbance drifts do not result from southward IMF Bz driven prompt penetration electric fields. SAPS have recently also been associated with equatorial electrojet disturbance dynamo effects (Zhang K. et al., 2021).

2.7 Disturbance dynamo effects

The disturbance dynamo mechanism (Blanc and Richmond, 1980; Scherliess and Fejer, 1997) is the dominant driver of low latitude low latitude electric field and current perturbations in the recovery phase of geomagnetic storms. Fejer et al. (2017) reviewed their causes and recent results on their middle and low latitude electrodynamic effects. Navarro et al. (2019) showed that over Jicamarca the average disturbance dynamo vertical drifts are downward and generally small during daytime. Pandey et al. (2018) suggested that, in presence of a favorable semidiurnal tidal component (particularly during equinoctial months in high solar activity period), the disturbance dynamo related electric field perturbations during daytime can be as large as at nighttime. Near dusk, the disturbance dynamo vertical drifts are downward, have largest values during the autumnal equinox, smallest during May-June, and increase strongly with solar flux and enhanced geomagnetic activity (e.g., Fejer, 2002). At night, they are upward, do not change much with season, and increase with solar flux and geomagnetic activity (Navarro et al., 2019). The zonal disturbance dynamo drifts are eastward during the day and westward at night with generally largest values near midnight (e.g., Fejer et al., 2005; Navarro and Fejer, 2020).

Disturbance dynamo and prompt penetration electric fields have also been studied recently using the magnetic response of

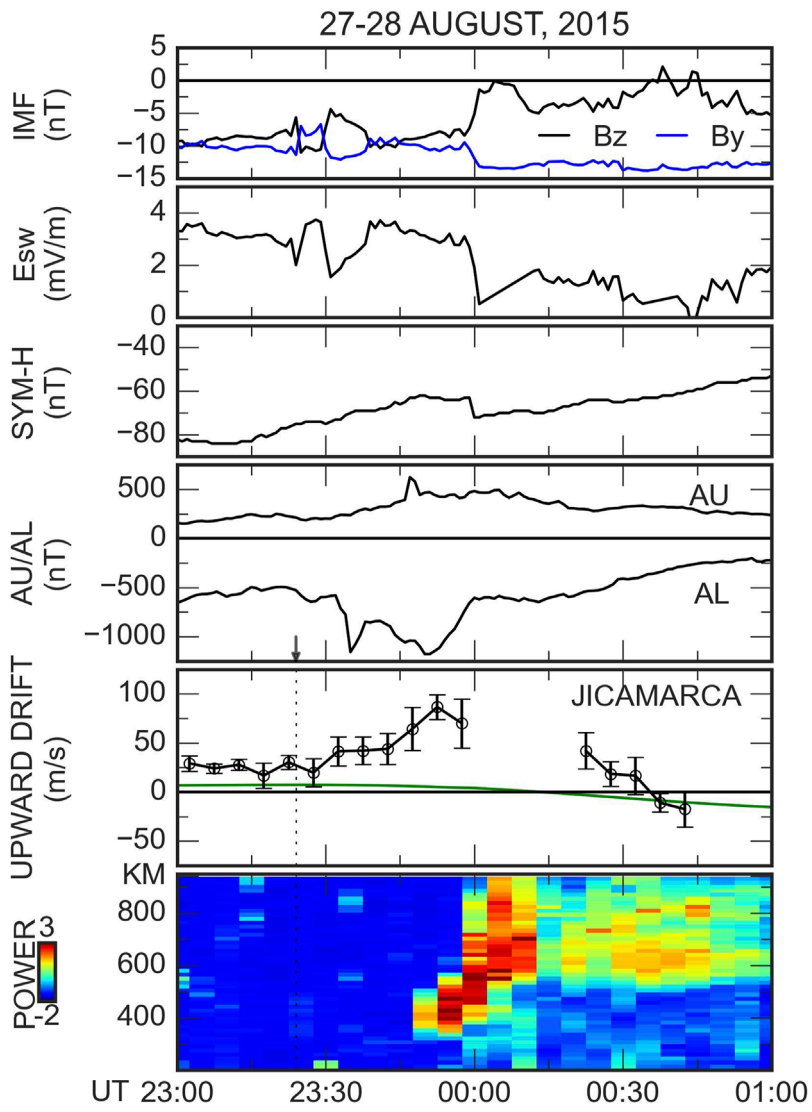

FIGURE 3
Solar wind and magnetospheric indices, average Jicamarca vertical drifts and coherent backscattered power during August 27–28, 2015. The green line corresponds to the quiet drift pattern. The errors bars denote the standard deviations of the drifts. Over Jicamarca UT = LT + 5 h. Adapted from Fejer et al., 2021.

their equivalent current systems (e.g., Rodriguez-Zuluaga et al., 2016; Bulusu et al., 2018; Younas et al., 2021). The disturbance dynamo magnetic signatures, the so-called Ddyn (e.g., Le Huy and Amory-Mazaudier, 2005; Amory-Mazaudier et al., 2017), appear as storm-time negative geomagnetic field excursions relative to their diurnal quiet time values, i.e., as anti-Sq circulations. Rodriguez-Zuluaga et al. (2016) reported good agreement between Equatorial Ionization Anomaly (EIA) and disturbance dynamo parameters during high-speed solar wind stream (HSSW), but not during coronal mass ejection (CME) events. Younas et al. (2021) showed that D_{dyn} is longest lasting during equinox, and that HSSW generated D_{dyn} occur globally and generally last longer than the more localized CME) generated D_{dyn}.

3 Equatorial ionospheric electrodynamics during the December 2006 large geomagnetic storm

The CME driven 14–15 December 2006 large geomagnetic storm started at ~1414 UT with a large shock as a result of the sudden increase in the solar wind speed from 650 to 980 km/s. After the shock, the solar wind speed underwent a gradual decrease but remained above 600 km/s for most of this long-lasting storm. The storm main phase started at ~2310 UT on14th following the IMF Bz rapid southward turning. Lei et al. (2008), Wang et al. (2008) used Coupled Magnetosphere Ionosphere Thermosphere (CMIT) model simulations to study the thermospheric and ionospheric response to the initial phase (~8 h) of this

storm. Veenadhari et al. (2019) examined substorm electrodynamic signatures during this storm and Ranjan et al. (2023) studied this storm-driven ionospheric variability over the Indian sector.

Figure 4 shows in the top 5 panels the ACE satellite measured IMF Bz/By and motional electric field (positive duskward), and the SMR, SMU, SML geomagnetic indices from 00 UT to 10 UT on 15 December. The next two panels present the equatorial electrojet data over Micronesia and India determined from the difference of the magnetic field horizontal components over Yap (9.6°N, 138.1°E) and Okinawa (26.3°N, 127.8°E) and Tirunelveli (8.7°N, 77.8°E) and Alibag (18.7°N, 72.9°E), respectively (Veenadhari et al., 2019). The bottom panels show the vertical drift velocity and backscattered power from 3-m plasma irregularities measured by the JULIA probe. Over the ~120–160 km height range, these drifts are the nighttime equivalents to the daytime so-called 150 km drifts. The power from the ~110 km region results from the backscatter of electrojet two-stream and gradient-drift plasma irregularities (e.g., Fejer and Kelley, 1980). Height changes in the electrojet backscattered power are indicative of zonal electric field reversals and occurrence of gradient drift plasmas irregularities.

Figure 4 indicates that following the main phase onset, the IMF Bz remained southward for several hours, except for brief northward excursions at ~0520 UT. The IMF By oscillated up to 00 UT on the 15th, increased to ~10 nT to ~06 UT, and then decreased to ~5 nT. The solar wind dynamic pressure (not shown) was very small after ~01 UT. The SMR went down to −163 nT at 0055 UT, and the SMU and SML had peak values ~1,000 and ~2,400 nT, respectively. Over this period, the SuperMAG website lists 20 substorm onsets based on the Newell and Gjerloev (2011) criteria.

The solar wind, auroral electrojet, ring current, storm-time equatorial electrojet data, and complementary geosynchronous particle flux measurements from LANL (Los Alamos National Laboratory) satellites (not shown) during this event were discussed in detail by Veenadhari et al. (2019). They pointed out that the sharp decrease in storm time electrojet at 0100 UT over the Japanese sector and at 0525 UT over the Indian sector, shown in Figure 4, were most likely due to change in solar wind dynamic pressure and sudden sharp IMF Bz northward turning, respectively. Figure 4 also shows particularly large decreases in the East Asian and Indian storm - time electrojet data between 0200 and 0400 UT when the solar wind dynamic pressure was low and steady, and the IMF Bz was southward and slowly changing. Veenadhari et al. (2019) pointed out that, over this period, LANL satellite dusk geosynchronous particle flux and Asymmetric-D and Asymmetric-H data indicated the occurrence of substorms. They suggested that these strong daytime overshieldings driving westward equatorial electrojet currents during the large southward IMF Bz can be interpreted as due to substorm driven increased Region 2 Field-Aligned Currents (R2 FACs) (e.g., Ebihara et al., 2014). Veenadhari et al., (2019) pointed out that this daytime overshielding does fit the standard disturbance dynamo signatures. On the other hand, we believe that disturbance dynamo effects cannot be fully ruled out.

The last two panels of Figure 4 show generally very strong upward drifts (often over 150 m/s) and electrojet backscattered power up to ~04 UT (23 LT) over Jicamarca. This is particularly the case during 02–04 UT when there was strong counter electrojet activity in the East Asian and Indian sectors. Over this period, h'F and hmF2 over Jicamarca reached over ~500 km (among the highest ever recorded), and the radar measurements showed very strong spread F activity, which will be discussed later. From ~04–08 UT, the Jicamarca data show large short-lived vertical drifts enhancements (overshieldings) with corresponding variations in the height and strength of the electrojet backscattered power. We associate these large vertical drift enhancements with the occurrence of strong substorms. After ~08 UT, there were there were no further upward drift enhancements, and the electrojet backscattered power became strong again, which is indicative of strong westward electric fields driven two-stream electrojet irregularities.

Figure 5 show highly structured early night equatorial 3-m plasma irregularities over Jicamarca rapidly expending to high latitudes as expected from the actions of the very strong and highly variable upward drifts shown in Figure 5, and consistent with elevated h'F and hmF2 values. The large structuring of the plasma irregularities is consistent with highly variable substorm associated vertical and zonal prompt penetration electric fields. The F-region irregularities and the electrojet backscattered power weakened significantly a about ~04 UT (23 LT) consistent with decrease of upward drifts. Later, the F-region irregularities systematically move downward in spite of occasional occurrence of upward drifts.

Huang C.-S. (2019) presented dusk-evening upward drifts of up to ~180 m/s measured by five DMSP satellites during 00–12 UT on 15 December 2006. These large upward drifts were interpreted as caused by continuous penetration of solar wind electric fields, in partial agreement with the radar data. The simultaneous occurrence of strong daytime overshielding, as indicated by the morning daytime electrojet data and evening and early night strong undershielding, as shown by the radar and DMSP data is not consistent with the expected prompt penetration electric field pattern (e.g., Fejer and Scherliess, 1997). We speculate that these apparently contradictory results might have been caused by strong rotations and/or skewing of the northern and southern high latitude convection patterns. The fundamental point highlighted by this Asian and South American data is that interpretations based on single site observations cannot be generalized to other longitudinal sectors. This clearly points to the need for multiple measurements at least during major magnetic storms.

4 Recent modeling studies

Magnetic-field aligned currents driven global convection changes (e.g., Wolf, 1970) often give rise to strong global electron electrodynamic perturbations (e.g., Nishida el al., 1966; Kelley et al., 1979; Fejer, 2011; Kikuchi, 2021). The basic characteristics of storm time driven low latitude short and longer lasting low latitude electrodynamic perturbations have been largely explained by numerous theoretical and numerical more than 2 decades ago (e.g., Blanc and Richmond, 1980; Senior and Blanc, 1984; Spiro et al., 1988; Sazykin, 2000; Richmond et al., 2003; Maruyama et al., 2011). However, these models did not accurately account for the coupling of the magnetosphere to the ionosphere and thermosphere, which made it particularly difficult to accurately simulate penetrating electric fields (e.g., Lu et al., 2012). Recently, Lu et al. (2020) showed that the TIEGCM driven by realistic storm-time magnetospheric forcing was able to reproduce many observed large-scale ionospheric features during 17 March 2015 storm determined from GNSS

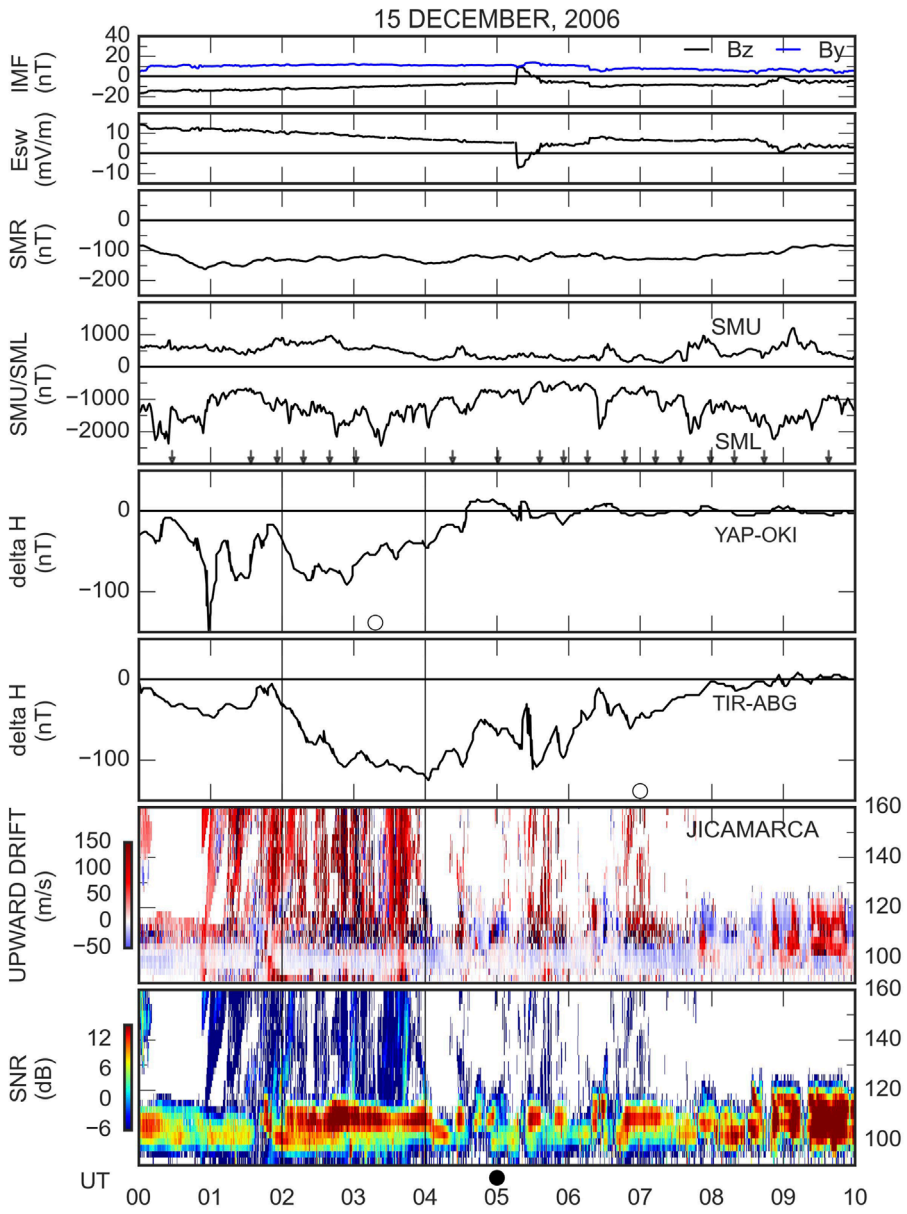

FIGURE 4
(Top four panels) Solar wind IMF Bz/By and motional east-west electric field, and SuperMAG ring current (SMR) and auroral current (SMU/SML) indices with and substorm onset times (small arrows). (Fifth and sixth panels) Equatorial electrojet magnetic fields data from the East Asian and Indian sectors (adapted from Veenadhari et al., 2019). (Bottom two panels) Jicamarca vertical plasma drifts and backscattered power from 3-m plasma irregularities. The open and full circles denote local noon and midnight, respectively.

TEC data. Although no comparisons were made with measured low latitude electric fields and currents, the modelled equatorial prompt penetration electric fields, in response to a rapid IMF southward excursion, were consistent with their expected patterns. Maute et al. (2021) presented TIEGCM simulations of hemispheric asymmetric electric potential using the Weimer electric potential, the Assimilative Mapping of Ionospheric Electrodynamics (AMIE) derived electric potential, and auroral parametrization from field-aligned currents based on AMPERE data. The simulated equatorial electric fields using the different potentials were generally consistent with each other and with expected patterns during daytime, but not near dawn and dusk. Recently, Wu et al. (2024) reported simulations of prompt penetration electric field during the initial phase of the 3–4 November 2021 using the recently developed Multiscale Atmosphere-Geospace Environment (MAGE) mode MAGE that are generally consistent with measurements from the Ionospheric Connection Explorer (ICON) satellite. MAGE, which combines a MHD (Magnetohydrodynamics), the Rice Convection Model (RCM) of the ring current, and the TIEGCM models (e.g., Lin et al., 2022; Wu et al., 2024), has a faster high latitude driver for the ionosphere thermosphere models allowing for more realistic simulations of SAPS and prompt

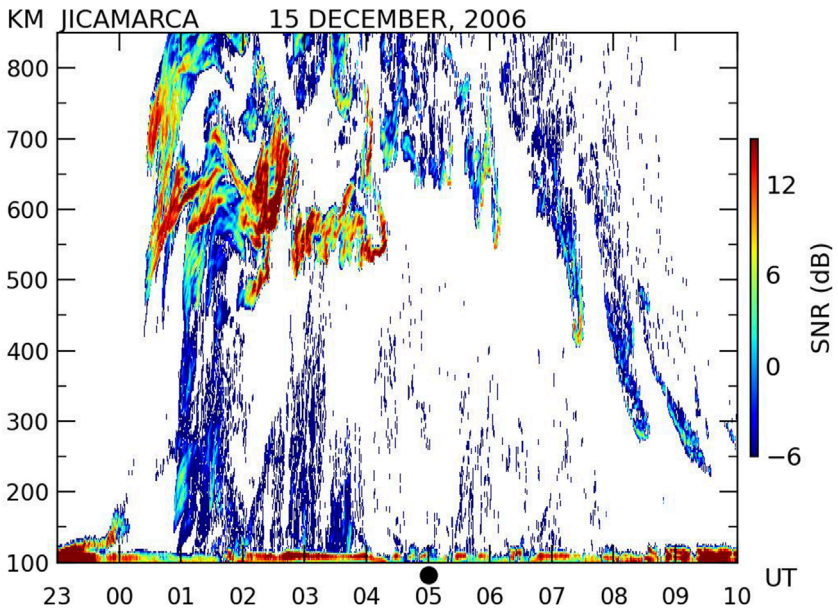

FIGURE 5
Backscattered power from 3-m plasma irregularities over Jicamarca during the 15 December 2006 geomagnetic storm. The full circle denotes local midnight.

penetration electric fields. Hopefully, storm-time simulations using these upgraded models will be extended down to low latitudes more often.

5 Summary and suggestions for future studies

We have seen that, over the last 2 decades, several studies examined the roles of solar wind, magnetosphere and high latitude ionospheric processes in driving geomagnetically active low latitude electrodynamics (e.g., Fejer, 2011; Tulasi Ram et al., 2012; Fejer et al., 2024; Wu et al., 2024; Chakrabarty et al., 2015; 2017; Huang C.-S. 2020a; b; Li et al., 2023; Wang and Luhr, 2024). They reported initial results on complex longitude dependent electrodynamic responses caused by simultaneous multiple disturbance drivers, IMF By convection rotations and skewing, long lasting substorm activity, and season dependent interhemispheric asymmetries. At present, the most pressing outstanding questions revolve around the roles of IMF By sign and season and hemispheric dependent convection pattern changes. These processes play particularly important roles on low latitude electrodynamic processes near dawn and dusk. Additional very important remaining questions include the conditions for the occurrence of very large amplitude substorms near dusk and possibly also near dawn, and of large amplitude overshielding driven by region 2 field-aligned current under slowly varying southward IMF Bz. Overall, however, the main challenge is how to account for the short- and -longer term effects of these very diverse solar wind, magnetosheric, and high latitude parameters.

Significantly more extensive comprehensive ground-based and *in-situ* satellite measurements are required for detailed studies of the above questions. In terms of ground-based data, additional routine measurements of ionospheric electrodynamics parameters over Africa and Asia are particularly desirable. The use of common parameters would greatly improve the study of low latitude electrodynamics during quiet and disturbed conditions. For instance, equatorial electrojet magnetic field measurements converted into vertical plasma drifts (i.e., zonal electric fields) using the dual magnetometer procedure developed by Anderson et al. (2002) would greatly facilitate comparisons with ground-based electrojet, radar and satellite electric field measurements. Since convection patterns changes appear increasingly important for low latitude studies, significantly more frequent use of northern and southern SuperDARN and other high and middle latitude measurements and low latitude data is clearly desirable.

The development of effective predictive models is the ultimate objective of space weather research. The development of increasingly comprehensive models like MAGE is a significant step forward towards this objective. MAGE simulations routinely extended to low latitudes would greatly improve low latitude electrodynamics studies. In the meantime, simulations studies with models like the TIEGCM and RCM, even with idealized input parameters, can help to improve the understanding of the effects of different physical processes and also can guide experimental studies in singling out the effects of different driving parameters. The recent experimental and modeling studies indicate the strong continued interest in the study of solar wind/magnetosphere low latitude coupling and their electrodynamic effects.

Author contributions

BF: Writing–original draft, Writing–review and editing. Luis A LN: Writing–review and editing. DC: Writing–review and editing.

Funding

The author(s) declare that financial support was received for the research, authorship, and/or publication of this article. LN was supported by NASA-ECIP award #80NSSC23K1066. The work of DC is supported by the Department of Space, Government of India. The Jicamarca Radio Observatory is a facility of the Instituto Geofisico del Perú operated with support from NSF award AGS-1732209 through Cornell University.

Acknowledgments

We thank the Jicamarca staff and for the radar observations. The Jicamarca Radio Observatory is a facility of the Instituto Geofisico del Perú operated with support from NSF award AGS-1732209 through Cornell University. We acknowledge the substorm timing list identified by the Newell and Gjerloev technique (Newell and Gjerloev, 2011), the SMU and SML indices (Newell and Gjerloev, 2011); and the SuperMAG collaboration (Newell and Gjerloev, 2011). LN was supported by NASA-ECIP award #80NSSC23K1066.

Conflict of interest

The authors declare that the research was conducted in the absence of any commercial or financial relationships that could be construed as a potential conflict of interest.

Publisher's note

References

Abdu, M. A. (2016). Electrodynamics of ionospheric weather over low latitudes. *Geos. Lett.* 3, 11–13. doi:10.1186/s40562-016-0043-6

Abdu, M. A., Maruyama, T., Batista, I. S., Saito, S., and Nakamura, M. (2007). Ionospheric responses to the October 2003 superstorm: longitude/local time effects over equatorial low and middle latitudes. *J. Geophys. Res.* 112, A10306. doi:10.1029/2006JA012228

Amory-Mazaudier, C., Bolaji, O. S., and Doumbia, V. (2017). On the historical origins of the CEJ, DP2, and Ddyn current systems and their roles in the predictions of ionospheric responses to geomagnetic storms at equatorial latitudes. *J. Geophys. Res. Space Phys.* 122, 7827–7833. doi:10.1002/2017JA024132

Anderson, D., Anghel, A., Yumoto, K., Ishitsuka, M., and Kudeki, E. (2002). Estimating daytime vertical ExB drift velocities in the equatorial F-region using ground-based magnetometer observations. *Geophys. Res. Lett.* 29 (12), 37–41. doi:10.1029/2001gl014562

Bagiya, M. S., Hazarika, R., Laskar, F. I., Sunda, S., Gurubaran, S., Chakrabarty, D., et al. (2014). Effects of prolonged southward interplanetary magnetic field on low-latitude ionospheric electron density. *J. Geophys. Res. Space Phys.* 119, 5764–5776. doi:10.1002/2014JA020156

Balan, N., Thampi, S. V., Lynn, K., Otsuka, Y., Alleyne, H., Watanabe, S., et al. (2008). F3 layer during penetration electric field. *J. Geophys. Res.* 113, A00A07. doi:10.1029/2008JA013206

Baumjohann, W., Kamide, Y., and Nakamura, R. (1996). Substorms, storms, and the near-Earth tail. *J. Geomagn. Geoelectr.* 48, 177–185. doi:10.5636/jgg.48.177

Bhaskar, A., and Vichare, G. (2013). Characteristics of penetration electric fields to the equatorial ionosphere during southward and northward IMF turnings. *J. Geophys. Res. Space Phys.* 118, 4696–4709. doi:10.1002/jgra.50436

Blanc, M., and Richmond, A. D. (1980). The ionospheric disturbance dynamo. *J. Geophys. Res.* 85 (A4), 1669–1686. doi:10.1029/JA085iA04p01669

Bulusu, J., Chandrasekhar, N. P., and Nagarajan, N. (2018). Effect of disturbance electric fields on equatorial electrojet over Indian longitudes. *J. Geophys. Res. Space Phys.* 123, 5894–5916. doi:10.1029/2018JA025247

Caan, N. N., McPheron, R. L., and Russel, C. T. (1977). Characteristics of the association between interplanetary magnetic field and substorms. *J. Geophys. Res.* 82 (29), 4837–4842. doi:10.1029/JA082i029p04837

Chakrabarty, D., Hui, D., Rout, D., Sekar, R., Bhattacharyya, A., Reeves, G. D., et al. (2017). Role of IMF b_y in the prompt electric field disturbances over equatorial ionosphere during a space weather event. *J. Geophys. Res. Space Phys.* 122, 2574–2588. doi:10.1002/2016JA022781

Chakrabarty, D., Rout, D., Sekar, R., Narayanan, R., Reeves, G. D., Pant, T. K., et al. (2015). Three different types of electric field disturbances affecting equatorial ionosphere during a long-duration prompt penetration event. *J. Geophys. Res. Space Phys.* 120, 4993–5008. doi:10.1002/2014JA020759

Chakrabarty, D., Sekar, R., Narayanan, R., Patra, A. K., and Devasia, C. V. (2006). Effects of interplanetary electric field on the development of an equatorial spread f event. *J. Geophys. Res.* 111, A12316. doi:10.1029/2006JA011884

Chakrabarty, D., Sekar, R., Sastri, J. H., Pathan, B. M., Reeves, G. D., Yumoto, K., et al. (2010). Evidence for oi 630.0 nm dayglow variations over low latitudes during onset of a substorm. *J. Geophys. Res.* 115, A10316. doi:10.1029/2010JA015643

Chakrabarty, D., Sekar, R., Sastri, J. H., and Ravindran, S. (2008). Distinctive effects of interplanetary electric field and substorm on nighttime equatorial f layer: a case study. *Geophys. Res. Lett.* 35, L19108. doi:10.1029/2008GL035415

Chakraborty, S., and Chakrabarty, D. (2023). Global asymmetry in ΔX variations during the 06 April 2000 geomagnetic storm: relative roles of IMF B_z and b_y. *J. Geophys. Res. Space Phys.* 128. doi:10.1029/2022JA031047

Chen, J., Lei, J., Wang, W., Liu, J., Maute, A., Qian, L., et al. (2021). Electrodynamical coupling of the Geospace system during solar flares. *J. Geophys. Res. Space Phys.* 126. doi:10.1029/2020JA028569

Cowley, S. W. H. (1981). Magnetospheric asymmetries associated with the y-component of the IMF. *Planet. Space Sci.* 29, 79–96. doi:10.1016/0032-0633(81)90141-0

Cowley, S. W. H., Morelli, J. P., and Lockwood, M. (1991). Dependence of convective flows and particle precipitation in the high-latitude dayside ionosphere on the X and Y components of the interplanetary magnetic field. *J. Geophys. Res.* 96, 5557–5564.

Cumnock, J. A., Heelis, R. A., and Hairston, M. R. (1992). Response of the ionospheric convection pattern to a rotation of the interplanetary magnetic field on January 14, 1988. *J. Geophys. Res. Space Phys.* 97 (A12), 19449–19460. doi:10.1029/92ja01731

Ebihara, Y., Tanaka, T., and Kikuchi, T. (2014). Counter equatorial electrojet and overshielding after substorm onset: global MHD simulation study. *J. Geophys. Res.* 119 (9), 7281–7296. doi:10.1002/2014JA020065

Fagundes, P. R., Cardoso, F. A., Fejer, B. G., Venkatesh, K., Ribeiro, B. A. G., and Pillat, V. G. (2016). Positive and negative GPS-TEC ionospheric storm effects during the extreme space weather event of March 2015 over the Brazilian sector. *J. Geophys. Res. Space Phys.* 121 (6), 5613–5625. doi:10.1002/2015JA022214

Fejer, B. G. (1997). The electrodynamics of the low latitude ionosphere: recent results and future challenges. *J. Atmos. Sol. Terr. Phys.* 59, 1465–1482. doi:10.1016/s1364-6826(96)00149-6

Fejer, B. G. (2002). Low latitude storm time ionospheric electrodynamics. *J. Atmos. Sol. Terr. Phyics.* 64, 1401–1408. doi:10.1016/s1364-6826(02)00103-7

Fejer, B. G. (2011). Low latitude ionospheric electrodynamics. *Space Sci. Rev.* 158 (1), 145–166. doi:10.1007/s11214-010-9690-7

Fejer, B. G., Blanc, M., and Richmond, A. D. (2017). Post-storm middle and low-latitude ionospheric electric fields effects. *Space Sci. Rev.* 206, 407–429. doi:10.1007/s11214-016-0320-x

Fejer, B. G., and Emmert, J. T. (2003). Low-latitude ionospheric disturbance electric field effects during the recovery phase of the 19 – 21 October 1998 magnetic storm. *J. Geophys. Res.* 108 (A12), 1454. doi:10.1029/2003JA010190

Fejer, B. G., Jensen, J. W., Kikuchi, T., Abdu, M. A., and Chau, J. L. (2007). Equatorial ionospheric electric fields during the November 2004 magnetic storm. *J. Geophys. Res.* 112 (A10). doi:10.1029/2007JA012376

Fejer, B. G., Jensen, J. W., and Su, S. (2008). Seasonal and longitudinal dependence of equatorial disturbance vertical plasma drifts. *Geophys. Res. Lett.* 35, L20106. doi:10.1029/2008gl035584

Fejer, B. G., and Kelley, M. C. (1980). Ionospheric irregularities. *Rev. Geophys.* 18 (2), 401–454. doi:10.1029/rg018i002p00401

Fejer, B. G., Laranja, S. R., and Condor, P. (2024). Multi-process driven unusually large equatorial perturbation electric fields during the April 2023 geomagnetic storm. *Front. Astron. Space Sci.* 11, 1351735. doi:10.3389/fspas.2024.1351735

Fejer, B. G., and Maute, A. (2021). Equatorial ionospheric electrodynamics. *Ionos. Dyn. Appl.*, 159–183. doi:10.1002/9781119815617.ch9

Fejer, B. G., and Navarro, L. A. (2022). First observations of equatorial ionospheric electric fields driven by storm-time rapidly recurrent magnetospheric substorms. *J. Geophys. Res. Space Phys.* 127 (12), e2022JA030940. doi:10.1029/2022ja030940

Fejer, B. G., Navarro, L. A., Sazykin, S., Newheart, A., Milla, M., and Condor, P. (2021). Prompt penetration and substorm effects over Jicamarca during the september 2017 geomagnetic storm. *J. Geophys. Res. Space Phys.* 126 (8), 1–11. doi:10.1029/2021JA029651

Fejer, B. G., and Scherliess, L. (1997). Empirical models of storm time equatorial zonal electric fields. *J. Geophys. Res.* 102 (A11), 24047–24056. doi:10.1029/97JA02164

Fejer, B. G., Scherliess, L., and de Paula, E. R. (1999). Effects of the vertical plasma drift velocity on the generation and evolution of equatorial spread F. *J. Geophys. Res. Space Phys.* 104 (A9), 19859–19869. doi:10.1029/1999JA900271

Fejer, B. G., Souza, J. R., Santos, A. S., and Costa Pereira, A. E. (2005). Climatology of F region zonal plasma drifts over Jicamarca. *J. Geophys. Res. Space Phys.* 110, A12310. doi:10.1029/2005JA011324

Fejer, B. G., Spiro, R. W., Wolf, R. A., and Foster, J. C. (1990). Latitudinal variation of perturbation electric fields during magnetically disturbed periods: 1986 SUNDIAL observations and model results. *Ann. Geophys.* 8 (6), 441–454.

Foster, J. C., and Burke, W. J. (2002). SAPS: a new categorization for sub-auroral electric fields. *EOS Trans. Am. Geophys Union* 83, 393–394. doi:10.1029/2002EO000289

Foster, J. C., and Vo, H. B. (2002). Average characteristics and activity dependence of the subauroral polarization stream. *J. Geophys. Res.* 107 (A12), 1475. doi:10.1029/2002JA009409

Friis-Christensen, E., Kamide, Y., Richmond, A. D., and Matsushita, S. (1985). Interplanetary magnetic field control of high-latitude electric fields and currents determined from Greenland magnetometer data. *J. Geophys. Res. Space Phys.* 90 (A2), 1325–1338. doi:10.1029/ja090ia02p01325

Friis-Christensen, E., Lassen, K., Wilhjelm, J., Wilcox, J. M., Gonzalez, W., and Colburn, D. S. (1972). Critical component of the interplanetary magnetic field responsible for large geomagnetic effects in the polar cap. *J. Geophys. Res.* 77 (19), 3371–3376. doi:10.1029/ja077i019p03371

Fuller-Rowell, T. J., Richmond, A. D., and Maruyama, N. (2008). "Global modeling of storm-time thermospheric dynamics and electrodynamics," in *Midlatitude ionospheric dynamics and disturbances*. Editors P. M. Kintner, A. J. Coster, T. Fuller-Rowell, A. J. Mannucci, M. Mendillo, and R. Heelis, 187–200. (Am. Geophys. Union Geophysical Monograph 181, 2008.

Galperin, Y., Ponomarev, V. N., and Zosimova, A. G. (1974). Plasma convection in the polar ionosphere. *Ann. Geophys.* 30, 1.

Gao, S., Cai, H., Zhan, W., Wan, X., Xiong, C., Zhang, H., et al. (2023). Characterization of local time dependence of equatorial spread F responses to substorms in the American sector. *Space Weather Space Clim.* 13, 2. doi:10.1051/swsc/2022039

Garner, T. W., Wolf, R. A., Spiro, R. W., Burke, W. J., Fejer, B. G., Sazykin, S., et al. (2004). Magnetospheric electric fields and plasma sheet injection to low L-shells during the 4–5 June 1991 magnetic storm: Comparison between the Rice Convection Model and observations. *J. Geophys. Res.* 109 (A02). doi:10.1029/2003JA010208

Heelis, R. A. (1984). The effects of interplanetary magnetic field orientation on dayside high latitude ionospheric convection. *J. Geophys. Res. Space Phys.* 89 (A5), 2873–2880. doi:10.1029/ja089ia05p02873

Heelis, R. A., and Maute, A. (2020). Challenges to understanding the Earth's ionosphere and thermosphere. *J. Geophys. Res. Space Phys.* 125, e2019JA027497. doi:10.1029/2019JA027497

Holappa, L., and Buzulukova, N. Y. (2022). Explicit IMF b_y-dependence of Energetic Protons and the ring current. *Geophys. Res. Lett.* 49, e2022GL098031. doi:10.1029/2022gl098031

Huang, C.-S. (2009). Eastward electric field enhancement and geomagnetic positive bay in the dayside low-latitude ionosphere caused by magnetospheric substorms during sawtooth events. *Geophys. Res. Lett.* 36, L18102. doi:10.1029/2009GL040287

Huang, C.-S. (2012). Statistical analysis of dayside equatorial ionospheric electric fields and electrojet currents produced by magnetospheric substorms during sawtooth events. *J. Geophys. Res.* 117, A02316. doi:10.1029/2011JA017398

Huang, C.-S. (2015). Storm-to-storm main phase repeatability of the local time variation of disturbed low-latitude vertical ion drifts. *Geophys. Res. Lett.* 42, 5694–5701. doi:10.1002/2015GL064674

Huang, C.-S. (2019). Long-lasting penetration electric fields during geomagnetic storms: observations and mechanisms. *J. Geophys. Res. Space Phys.* 124, 9640–9664. doi:10.1029/2019JA026793

Huang, C.-S. (2020a). Systematical analyses of global ionospheric disturbance current systems caused by multiple processes: penetration electric fields, solar wind pressure impulses, magnetospheric substorms, and ULF waves. *J. Geophys. Res. Space Phys.* 125 (9), e2020JA027942. doi:10.1029/2020JA027942

Huang, C.-S. (2020b). Westward plasma drifts in the nighttime equatorial ionosphere during severe magnetic storms: a new type of penetration electric fields caused by subauroral polarization stream. *J. Geophys. Res. Space Phys.* 125, e2020JA028300. doi:10.1029/2020JA028300

Huang, C.-S., Rich, F. J., and Burke, W. J. (2010b). Storm time electric fields in the equatorial ionosphere observed near the dusk meridian. *J. Geophys. Res.* 115, A08313. doi:10.1029/2009JA015150

Huang, C.-S., Sazykin, S., Chau, J. L., Maruyama, N., and Kelley, M. C. (2007). Penetration electric fields: efficiency and characteristic time scale. *J. Atmos. Sol. Terr. Phys.* 69 (10-11), 1135–1146. doi:10.1016/j.jastp.2006.08.016

Huang, C.-S., Sazykin, S., Chau, J. L., Maruyama, N., and Kelley, M. C. (2010a). Penetration of electric fields: efficiency and characteristic time scale. *J. Atmos. Sol. Terr. Phys.* 69. doi:10.1016/j/jastp.2006.08.06

Huang, C.-S., Zhang, Y., Wang, W., Lin, D., and Wu, Q. (2021). Low-latitude zonal ion drifts and their relationship with subauroral polarization streams and auroral return flows during intense magnetic storms. *J. Geophys. Res. Space Phys.* 126, e2021JA030001. doi:10.1029/2021JA030001

Hui, D., Chakrabarty, D., Sekar, R., Reeves, G. D., Yoshikawa, A., and Shiokawa, K. (2017). Contribution of storm time substorms to the prompt electric field disturbances in the equatorial ionosphere. *J. Geophys. Res. Space Phys.* 122 (5), 5568–5578. doi:10.1002/2016JA023754

Kelley, M. C., Fejer, B. G., and Gonzales, C. A. (1979). An explanation for anomalous equatorial ionospheric electric fields associated with a northward turning of the interplanetary magnetic field. *Geophys. Res. Lett.* 6 (4), 301–304. doi:10.1029/GL006i004p00301

Kelley, M. C., and Makela, J. J. (2002). B_y dependent prompt penetrating electric fields at the magnetic equator. *Geophys. Res. Lett.* 29 (7), 571–573. doi:10.1029/2001GL014468

Kelley, M. C., Makela, J. J., Chau, J. L., and Nicolls, M. J. (2003). Penetration of the solar wind electric field into the magnetosphere/ionosphere system. *Geophys. Res. Lett.* 30 (4), 1158. doi:10.1029/2002GL016321

Kikuchi, T. (2021). Penetration of the magnetospheric electric fields to the low latitude ionosphere. *Ionos. Dyn. Appl.*, 313–338. doi:10.1002/9781119815617.ch14

Kikuchi, T., Hashimoto, K., and Nozaki, K. (2008). Penetration of magnetospheric electric fields to the equator during a geomagnetic storm. *J. Geophys. Res.* 113, A062. doi:10.1029/2007JA012628

Kikuchi, T., and Hashimoto, K. K. (2016). Transmission of the electric fields to the low latitude ionosphere in the magnetosphere-ionosphere current circuit. *Geosci. Lett.* 3, 4. doi:10.1186/s40562-016-0035-6

Kikuchi, T., Hashimoto, K. K., Kitamura, T.-I., Tachihara, H., and Fejer, B. (2003). Equatorial counterelectrojets during substorms. *J. Geophys. Res. Space Phys.* 108 (A11), 1406. doi:10.1029/2003JA009915

Kuai, J., Liu, L., Lei, J., Liu, J., Zhao, B., Chen, Y., et al. (2017). Regional differences of the ionospheric response to the July 2012 geomagnetic storm. *J. Geophys. Res. Space Phys.* 122 (4), 4654–4668. doi:10.1002/2016ja023844

Kumar, A., Chakrabarty, D., Fejer, B. G., Reeves, G. D., Rout, D., Sripathi, S., et al. (2023). A case of anomalous electric field perturbations in the equatorial ionosphere during postsunset hours: Insights. *J. Geophys. Res. Space Phys.* 128, e2022JA030826. doi:10.1029/2022JA030826

Laundal, K. M., and Østgaard, N. (2009). Asymmetric auroral intensities in the Earth's Northern and Southern hemispheres. *Nature* 460 (7254), 491–493. doi:10.1038/nature08154

Le, G., Liu, G., Yizengaw, E., Wu, C. C., Zheng, Y., Vines, S., et al. (2024). Responses of field-aligned currents and equatorial electrojet to sudden decrease of solar wind dynamic pressure during the March 2023 geomagnetic storm. *Geophys. Res. Lett.* 51 (10), e2024GL109427. doi:10.1029/2024gl109427

Le Huy, M., and Amory-Mazaudier, C. (2005). Magnetic signature of the ionospheric disturbance dynamo at equatorial latitudes: "D_{dyn}". *J. Geophys. Res.* 110, A10301. doi:10.1029/2004JA010578

Lei, J., Wang, W., Burns, A. G., Solomon, S. C., Richmond, A. D., Wiltberger, M., et al. (2008). Observations and simulations of the ionospheric and thermospheric response to the December 2006 geomagnetic storm: initial phase. *J. Geophys. Res.* 113, A01314. doi:10.1029/2007JA012807

Li, Q., Li, S., Chen, J., Liu, J., Zhang, R., Liu, L., et al. (2023). Polar and equatorial ionospheric electrodynamical coupling under a prolonged northward B_z interval. *J. Geophys. Res. Space Phys.* 128, e2023JA032079. doi:10.1029/2023JA032079

Lin, D., Wang, W., Merkin, V. G., Huang, C., Oppenheim, M., Sorathia, K., et al. (2022). Origin of dawnside subauroral polarization streams during major geomagnetic storms. *AGU Adv.* 3, e2022AV000708. doi:10.1029/2022AV000708

Liou, K., Sotirelis, T., and Gjerloev, J. (2017). Statistical study of polar negative magnetic bays driven by interplanetary fast-mode shocks. *J. Geophys. Res. Space Phys.* 122, 7463–7472. doi:10.1002/2017JA024465

Liou, K., Sotirelis, T., and Mitchell, E. (2020). Control of the east-west component of the interplanetary magnetic field on the occurrence of magnetic substorms. *Geophys. Res. Lett.* 47, e2020GL087406. doi:10.1029/2020GL087406

Liou, K., Sotirelis, T., and Richardson, I. (2018). Substorm occurrence and intensity associated with three types of solar wind structure. *J. Geophys. Res. Space Phys.* 123, 485–496. doi:10.1002/2017JA024451

Liu, J., Liu, L., Nakamura, T., Zhao, B., Ning, B., and Yoshiwaka, A. (2014). A case study of ionospheric storm effects during long-lasting southward IMF *z*-driven geomagnetic storm. *J. Geophys. Res.* 119, 7716–7731. doi:10.1002/2014JA020273

Lu, G., Goncharenko, L., Nicolls, M. J., Maute, A., Coster, A., and Paxton, L. J. (2012). Ionospheric and thermospheric variations associated with prompt penetration electric fields. *J. Geophys. Res.* 117, A08312. doi:10.1029/2012JA017769

Lu, G., Zakharenkova, I., Cherniak, I., and Dang, T. (2020). Large-scale ionospheric disturbances during the 17 March 2015 storm: a model-data comparative study. *J. Geophys. Res. Space Phys.* 125, e2019JA027726. doi:10.1029/2019JA027726

Manoj, C., and Maus, S. (2012). A real-time forecast service for the ionospheric equatorial zonal electric field. *Space weather.* 10, S09002. doi:10.1029/2012sw000825

Maruyama, N., Fuller-Rowell, T., Codrescu, M. V., Anderson, D., Richmond, A. D., Maute, A., et al. (2011) "Modeling the storm time electrodynamics," in *Aeronomy of the Earth's Atmosphere and ionosphere*. Editors M. A. Abdu, D. Pancheva, and A. Bhattacharyya (Dordrecht: Springer), 455–464.

Maute, A., Richmond, A. D., Lu, G., Knipp, D. J., Shi, Y., and Anderson, B. (2021). Magnetosphere-ionosphere coupling via prescribed field-aligned current simulated by the TIEGCM. *J. Geophys. Res. Space Phys.* 126, e2020JA028665. doi:10.1029/2020JA028665

Milan, S. E., Mooney, M. K., Bower, G., Fleetham, A. L., Vines, S. K., and Gjerloev, J. (2023). Solar wind-magnetosphere coupling during high-intensity long-duration continuous AE activity (HILDCAA). *J. Geophys. Res. Space Phys.* 128, e2023JA032027. doi:10.1029/2023JA032027

Navarro, L. A., and Fejer, B. G. (2020). Storm-time coupling of equatorial nighttime F region neutral winds and plasma drifts. *J. Geophys. Res. Space Phys.* 125 (9), e2020JA028253. doi:10.1029/2020ja028253

Navarro, L. A., Fejer, B. G., and Scherliess, L. (2019). Equatorial disturbance dynamo vertical plasma drifts over Jicamarca: Bimonthly and solar cycle dependence. *J. Geophys. Res. Space Phys.* 124 (6), 4833–4841. doi:10.1029/2019ja026729

Newell, P. T., and Gjerloev, J. W. (2011). Evaluation of SuperMAG auroral electrojet indices as indicators of substorms and auroral power. *J. Geophys. Res. Space Phys.* 116 (A12), A12211. doi:10.1029/2011JA016779

Newell, P. T., Sotirelis, T., Liou, K., Meng, C.-I., and Rich, F. J. (2007). A nearly universal solar wind-magnetosphere coupling function inferred from 10 magnetospheric state variables. *J. Geophys. Res.* 112, A01206. doi:10.1029/2006JA012015

Nilam, B., Ram, S. T., Shiokawa, K., Balan, N., and Zhang, Q. (2020). The solar wind density control on the prompt penetration electric field and equatorial electrojet. *J. Geophys. Res. Space Phys.* 125, e2020JA027869. doi:10.1029/2020JA027869

Nishida, A., and Jacobs, J. A. (1962). Equatorial enhancement of world-wide changes. *J. Geophys. Res.* 67, 4937–4940. doi:10.1029/jz067i012p04937

Østgaard, N., Laundal, K. M., Juusola, L., Åsnes, A., Håland, S. E., Weygand, J. M., et al. (2011). Inter hemispherical asymmetry of substorm onset locations and the interplanetary magnetic field. *Geophys. Res. Lett.* 38, L08104. doi:10.1029/2011GL046767

Østgaard, N., Mende, S. B., Frey, H. U., Immel, T. J., Frank, L. A., Sigwarth, J. B., et al. (2004). Interplanetary magnetic field control of the location of substorm onset and auroral features in the conjugate hemispheres. *J. Geophys. Res.* 109, A07204. doi:10.1029/2003JA010370

Pandey, K., Chakrabarty, D., and Sekar, R. (2018). Critical evaluation of the impact of disturbance dynamo on equatorial ionosphere during daytime. *J. Geophys. Res. Space Phys.* 123 (11), 9762–9774. doi:10.1029/2018ja025686

Pedatella, N. M., Chau, J. L., Vierinen, J., Qian, L., Reyes, P., Kudeki, E., et al. (2019). Solar flare effects on 150-km echoes observed over Jicamarca: WACCM-X simulations. *Geophys. Res. Lett.* 46, 10951–10958.

Qian, L., Burns, A. G., Solomon, S. C., and Chamberlin, P. C. (2012). Solar flare impacts on ionospheric electrodyamics. *Geophys. Res. Lett.* 39, L06101. doi:10.1029/2012GL051102

Ranjan, A. K., Sunil Krishna, M. V., Amory-Mazaudier, C., Fleury, R., Sripathi, S., Vichare, G., et al. (2023). Variability of ionosphere over Indian longitudes to a variety of space weather events during December 2006. *Space weather.* 21, e2023SW003595. doi:10.1029/2023SW003595

Reistad, J. P., Holappa, L., Ohma, A., Gabrielse, C., Sur, D., Asikainen, T., et al. (2022). Dependence of the global dayside reconnection rate on interplanetary magnetic field by and the earth's dipole tilt. *Front. Astronomy Space Sci.* 9, 973276. doi:10.3389/fspas.2022.973276

Richmond, A. D., Peymirat, C., and Roble, R. G. (2003). Long-lasting disturbances in the equatorial ionospheric electric field simulated with a coupled magnetosphere-ionosphere-thermosphere model. *J. Geophys. Res.* 118 (A3), 1118. doi:10.1029/2002JA009758

Rodríguez-Zuluaga, J., Radicella, S. M., Nava, B., Amory-Mazaudier, C., and Alazo-Cuartas, K. (2016). Distinct responses of the low-latitude ionosphere to CME and HSSWS: the role of the IMF B_z oscillation frequency. *J. Geophys. Res. Space Phys.* 121 (11), 528–548. doi:10.1002/2016JA022539

Rout, D., Chakrabarty, D., Sekar, R., Reeves, G. D., Ruohoniemi, J. M., Pant, T. K., et al. (2016). An evidence for prompt electric field disturbance driven by changes in the solar wind density under northward IMF *z* condition. *J. Geophys. Res. Space Phys.* 121, 4800–4810. doi:10.1002/2016JA022475

Rout, D., Pandey, K., Chakrabarty, D., Sekar, R., and Lu, X. (2019). Significant electric field perturbations in low latitude ionosphere due to the passage of two consecutive ICMEs during 6–8 September 2017. *J. Geophys. Res. Space Phys.* 124, 9494–9510. doi:10.1029/2019JA027133

Rout, D., Singh, R., Pandey, K., Pant, T., Stolle, C., Chakrabarty, D., et al. (2022). Evidence for presence of a global quasi-resonant mode of oscillations during high-intensity long-duration continuous AE activity (HILDCAA) events. *Earth Plan. Space* 74 (1), 91–11. doi:10.1186/s40623-022-01642-1

Sazykin, S. (2000). *Theoretical studies of penetration of magnetospheric electric fields to the ionosphere. ProQuest Dissertations and Theses Global*. Logan, UT: Utah State University.

Scherliess, L., and Fejer, B. G. (1997). Storm-time dependence of equatorial disturbance dynamo zonal electric fields. *J. Geophys. Res.* 102, 24037–24046. doi:10.1029/97JA02165

Senior, C., and Blanc, M. (1984). On the control of magnetospheric convection by the spatial distribution of ionospheric conductivities. *J. Geophys. Res.* 89 (A1), 261–284. doi:10.1029/JA089iA01p00261

Sori, T., Shinbori, A., Otsuka, Y., Tsugawa, T., Nishioka, M., and Yoshikawa, A. (2022). Generation mechanisms of plasma density irregularity in the equatorial ionosphere during a geomagnetic storm on 21–22 December 2014. *J. Geophys. Space Phys.* 127 (5), e2021JA030240. doi:10.1029/2021JA030240

Spiro, R. W., Heelis, R. A., and Hanson, W. B. (1979). Rapid subauroral ion drifts observed by Atmosphere Explorer C. *Geophys. Res. Lett.* 6, 657–660. doi:10.1029/gl006i008p00657

Spiro, R. W., Wolf, R. A., and Fejer, B. G. (1988). Penetration of high-latitude electric field effects to low latitude during SUNDIAL 1984. *Ann. Geophys.* 6, 39–50.

Tanaka, T., Nakamizo, A., Yoshikawa, A., Fujita, S., Shinagawa, H., Shimazu, H., et al. (2010). Substorm convection and current system deduced from the global simulation. *J. Geophys. Space Phys.* 115 (A5). doi:10.1029/2009JA014676

Tenfjord, P., Østgaard, N., Snekvik, K., Laundal, K. M., Reistad, J. P., Haaland, S., et al. (2015). How the IMF by induces a by component in the closed magnetosphere and how it leads to asymmetric currents and convection patterns in the two hemispheres. *J. Geophys. Res. Space Phys.* 120, 9368–9384. doi:10.1002/2015JA021579

Tsurutani, B. T., Lakhina, G. S., and Hajra, R. (2020). The physics of space weather/solar-terrestrial physics (STP): what we know now and what the current and future challenges are. *Nonlinear Process. Geophys.* 27, 75–119. doi:10.5194/npg-27-75-2020

Tsurutani, B. T., Verkhoglyadova, O. P., Mannucci, A. J., Saito, A., Araki, T., Yumoto, K., et al. (2008). Prompt penetration electric fields (PPEFs) and their ionospheric effects during the great magnetic storm of 30–31 October 2003. *J. Geophys. Res.* 113, A05311. doi:10.1029/2007JA012879

Tulasi Ram, S., Balan, N., Veenadhari, B., Gurubaran, S., Ravindran, S., Tsugawa, T., et al. (2012). First observational evidence for opposite zonal electric fields in equatorial E and F region altitudes during a geomagnetic storm period. *J. Geophys. Res.* 117, A09318. doi:10.1029/2012JA018045

Tulasi Ram, S., Yokoyama, T., Otsuka, Y., Shiokawa, K., Sripathi, S., Veenadhari, B., et al. (2016). Duskside enhancement of equatorial zonal electric field response to convection electric fields during the St. Patrick's Day storm on 17 March 2015. *J. Geophys. Res. Space Phys.* 121, 538–548. doi:10.1002/2015JA021932

Veenadhari, B., Kikuchi, T., Kumar, S., Ram, S. T., Chakrabarty, D., Ebihara, Y., et al. (2019). Signatures of substorm related overshielding electric field at equatorial latitudes under steady southward IMF Bz during main phase of magnetic storm. *Adv. Space Sci.* 64 (10), 1975–1988. doi:10.1016/j.asr.2019.04.001

Wang, H., and Lühr, H. (2024). IMF b_y effects on the strength and latitude of polar electrojets: CHAMP and Swarm Joint observations. *J. Geophys. Res. Space Phys.* 129, e2023JA032049. doi:10.1029/2023JA032049

Wang, W., Lei, J., Burns, A. G., Wiltberger, M., Richmond, A. D., Solomon, S. C., et al. (2008). Ionospheric electric field variations during a geomagnetic storm simulated by a coupled magnetosphere ionosphere thermosphere (CMIT) model. *Geophys. Res. Lett.* 35, L18105. doi:10.1029/2008GL035155

Wei, Y., Hong, M., Wan, W., Du, A., Lei, J., Zhao, B., et al. (2008). Unusually long lasting multiple penetration of interplanetary electric field to equatorial ionosphere under oscillating IMF B_z. *Geophs. Res. Lett.* 35, L02102. doi:10.1029/2007GL032305

Wei, Y., Pu, Z., Hong, M., Zong, Q., Ren, Z., Fu, S., et al. (2009). Westward ionospheric electric field perturbations on the dayside associated with substorm processes. *J. Geophys. Res.* 114, A12209. doi:10.1029/2009JA014445

Wei, Y., Wan, W., Zhao, B., Hong, M., Ridley, A., Ren, Z., et al. (2012). Solar wind density controlling penetration electric field at the equatorial ionosphere during a saturation of cross polar cap potential. *J. Geophys. Res.* 117, A09308. doi:10.1029/2012JA017597

Wei, Y., Zhao, B., Guozhu, L., and Wan, W. (2015). Electric field penetration into Earth's ionosphere: a brief review. *Sci. Bull.* 60 (8), 748–761. doi:10.1007/s11434-015-0749-4

Wolf, R. A. (1970). Effects of ionospheric conductivity on convective flow of plasma in the magnetosphere. *J. Geophys. Res.* 75 (25), 4677–4698. doi:10.1029/JA075i025p04677

Wolf, R. A., Harel, M., Spiro, R. W., Voigt, G.-H., and Chen, C.-K. (1982). Computer simulation of inner magnetospheric dynamics for the magnetic storm of July 29, 1977. *J. Geophys. Res.* 87 (A8), 5949–5962. doi:10.1029/JA087iA08p05949

Wolf, R. A., Spiro, R. W., Sazykin, S., and Toffoletto, F. R. (2007). How the Earth's inner magnetosphere works: an evolving picture. *J. Atmos. Sol. Terr. Phys.* 69 (3), 288–302. doi:10.1016/j.jastp.2006.07.026

Wu, Q., Wang, W., Lin, D., Huang, C., and Zhang, Y. (2024). Penetrating electric field during the Nov 3–4, 2021 geomagnetic storm. *J. Atmos. Sol. Terr. Phys.* 257, 106219. doi:10.1016/j.jastp.2024.106219

Xiong, C., Luhr, H., and Fejer, B. G. (2015). Global features of the disturbance winds during storm time deduced from CHAMP observations. *J. Geophys. Res. Space Phys.* 120, 5137–5150. doi:10.1002/2015JA021302

Yadav, S., Lyons, L. R., Nishimura, Y., Weygand, J. M., Liu, J., Zhang, S. R., et al. (2023). Association of equatorward extended auroral streamers with overshielding conditions at equatorial latitudes: first observations. *J. Geophys. Res. Space Phys.* 128 (11), e2023JA031726. doi:10.1029/2023ja031726

Yamazaki, Y., and Kosch, M. J. (2015). The equatorial electrojet during geomagnetic storms and substorms. *J. Geophys. Res. Space Phys.* 120, 2276–2287. doi:10.1002/2014ja020773

Yeh, H.-C., Foster, J. C., Rich, F. J., and W. Swider, W. (1991). Storm time electric field penetration observed at mid-latitude. *J. Geophys. Res.* 96, 5707–5721.

Younas, W., Amory-Mazaudier, C., Khan, M., and Le Huy, M. (2021). Magnetic signatures of ionospheric disturbance dynamo for CME and HSSWs generated storms. *Space weather.* 19, e2021SW002825. doi:10.1029/2021SW002825

Zhang, K., Wang, H., Yamazaki, Y., and Xiong, C. (2021). Effects of subauroral polarization streams on the equatorial electrojet during the geomagnetic storm on June 1, 2013. *J. Geophys. Res. Space Phys.* 126, e2021JA029681. doi:10.1029/2021JA029681

Zhang, R., Liu, L., Le, H., and Chen, Y. (2021). Equatorial ionospheric electrodynamics during solar flares. *Geophys. Res. Lett.* 44, 4558–4565. doi:10.1002/2017gl073238

Zhao, B., Wan, W., Liu, L., Igarashi, K., Nakamura, M., Paxton, L. J., et al. (2008). Anomalous enhancement of ionospheric electron content in the Asian-Australian region during a geomagnetically quiet day. *J. Geophys. Res.* 113, A11302. doi:10.1029/2007JA012987